J. Math. Biol. 48, 293–324 (2004)
Digital Object Identifier (DOI):
10.1007/s00285-003-0234-6

Mathematical Biology

Frithjof Lutscher · Mark A. Lewis

Spatially-explicit matrix models

A mathematical analysis of stage-structured integrodifference equations

Received: 23 August 2002 / Revised version: 12 March 2003 /

Abstract. This paper is concerned with mathematical analysis of the 'critical domain-size' problem for structured populations. Space is introduced explicitly into matrix models for stage-structured populations. Movement of individuals is described by means of a dispersal kernel. The mathematical analysis investigates conditions for existence, stability and uniqueness of equilibrium solutions as well as some bifurcation behaviors. These mathematical results are linked to species persistence or extinction in connected habitats of different sizes or fragmented habitats; hence the framework is given for application of such models to ecology. Several approximations which reduce the complexity of integrodifference equations are given. A simple example is worked out to illustrate the analytical results and to compare the behavior of the integrodifference model to that of the approximations.

1. Introduction

In the 'critical domain-size' problem for structured populations, reproduction and maturation of the structured population take place locally within an inhabitable patch or 'reserve', and loss from the inhabitable patch to uninhabitable exterior regions takes place due to dispersal across the patch boundary. This loss can be considered as a an 'edge effect' [9], where overall population growth is diminished due to boundary loss.

Whereas the total reproductive rate of the population scales with patch area, the dispersal loss scales with boundary length. Since surface area scales with the square of the linear dimension, boundary loss dominates dynamics of small patches but plays a diminished role in the dynamics of larger patches. The assumption that a small population grows in the absence of boundary loss leads to the existence of a critical size for the patch, below which the population cannot persist, and above which populations can grow. In turn, the critical domain-size provides a tool for reserve design and conservation [2,4].

A first model for critical domain-size in one space dimension, consisting of exponential population growth, Fickian diffusion, and a completely hostile exterior,

---

F. Lutscher, M.A. Lewis: Department of Mathematical and Statistical Sciences, University of Alberta, Edmonton, AB, Canada T6G 2G1.
e-mail: {flutscher;mlewis}@math.ualberta.ca

Key words or phrases: Integrodifference equations – Bifurcation analysis – Stage structure – Critical domain-size – Habitat fragmentation

was analyzed in [16] and [29]. These analyses have been extended to cover more complex spatial domains [30] and multiple interacting species [5]. Such models are formulated using assumptions of continuous-time reproduction and dispersal.

By way of contrast, in the absence of explicit spatial effects, stage- or age-structured matrix models have been the ‘work-horse’ for ecologists interested in population growth and persistence [6]. The single most important quantity in matrix models is the leading eigenvalue of the matrix. If it is greater than one, then the population can grow or persist. Matrix models have been applied in many different areas like fisheries [7], insects [15] or tree management [28], to name but a few.

The addition of dispersal into discrete-time models results in integrodifference equations [19]. It is appropriate if reproduction and dispersal occur as discrete non-overlapping events. In the scalar case, the critical domain-size problem has been analyzed in detail [32]. The more realistic case, which allows for both population and spatial structure and for stage-specific dispersal processes, is the stage-structured integrodifference model [26]. The purpose of this paper is to analyze the critical domain-size problem for the stage-structured integrodifference model, to provide the mathematical framework to study the effects of habitat fragmentation, and to derive approximations that link the analysis to the simpler matrix model case.

2. Modeling background

Simple difference equations of the form

$$u_{t+1} = f(u_t) = b(u_t)u_t \tag{1}$$

have been used widely to model the evolution of the density u_t of a population with discrete non-overlapping generations indexed by t. The function f describes the net effect of production of offspring and removal of individuals, and b stands for the per capita production minus mortality rate. Individuals are not differentiated with respect to age or stage. They are lumped together over the spatial domain in which the population lives, and environmental heterogeneity is neglected.

Extensions of (1) to stage-structured population models are written in matrix form

$$u(t+1) = F(u(t)) = B(u(t))u(t), \tag{2}$$

where now $u = (u_1, \dots, u_m)^T$ is the vector of densities of stages $1 \dots m$ and B is the matrix of net production rates. The entry b_{ij} is the net rate with which stage i is produced from stage j. The most comprehensive overview of the setup and application of these matrix models together with a detailed reference list can be found in [6]. Both model types, (1) and (2), exhibit a wide range of possible behavior from approaching equilibria or cycles to existence of strange attractors and chaotic behavior [6,18,31].

An extension of (1) to include spatial locations and movement of individuals assumes that population dynamics are governed by (1) and dispersal is governed by a probability density function or kernel $k(x, y)$ that describes the likelihood of jumping from y to x in a single time step. When growth and dispersal are separated in time, the integrodifference model results

$$u(t+1,x) = \int_\Omega k(x,y) f(u(t,y),y)dy, \tag{3}$$

where Ω denotes the domain of interest.

Although integrodifference models were initially formulated to study population genetics, recent applications have been made to ecological problems. One problem is the study of speeds of invasions and shapes of fronts. We will not address this question here, but give references for the sake of completeness [17,24,35,36]. Another problem regards critical domain-size and population persistence in fragmented habitats.

The first application of (3) to persistence in ecology was [19], where the model was derived, linear analysis was performed and the shapes of equilibrium solutions were studied numerically. Several aspects of density dependence and the possibility of pattern formation in homogeneous habitats were studied in [1]. A generalization of (3) to include temporal variation is given in a series of papers [11–13]. Existence and stability of fixed points and cycles were studied in the case where f varies periodically in time or even stochastically. Different dispersal strategies were compared with respect to persistence. The bifurcation structure of (3) was closely examined in [32]. An approximation for the spatial shape of the equilibrium solution in terms of the *dispersal success function* (see Section 5) was given. Persistence in a periodically varying heterogeneous domain was studied.

Much as the scalar model (1) can be extended to equation (3), the stage-structured model (2) can also be spatially extended. While this type of spatial stage-structured model has been used to model biological invasions [26], we are not aware of a systematic mathematical treatment of stage-structured integrodifference models for persistence in fragmented habitats. However, there is a growing interest amongst ecologists in applying such models, e.g., to reserve design [2].

The first goal of this paper is to thoroughly formulate stage-structured integrodifference models and to generalize the existence and bifurcation results of [32] (Section 3). In particular, Section 3.2.2 is somewhat technical and can be skipped at first. In Section 4, the theoretical results on the critical domain-size are illustrated with an example and numerical simulations. Then, several approximations are presented, which can be used to determine stationary solutions, their spatial shape and their stability without using excessive computer power or demanding large datasets (Section 5). Some effects of habitat fragmentation are discussed in Section 6. In Section 7, we extend part of the theory developed in Section 3 to the case where certain stages are sedentary. A table of the most frequently used symbols is included in appendix A.1.

3. Formulation and analysis of the model

3.1. Formulation

We assume that the non-spatial model (2) for a population with m stages and non-overlapping generations is given. To introduce space, we denote $\Omega \subset \mathbb{R}^n$ as the spatial domain of interest. We exclude all points from Ω where the population cannot settle and reproduce. We account for possibly varying conditions in the domain by allowing the matrix of production rates, $B(u, y)$, to depend on space explicitly. We assume that there is emigration from the domain but there is no immigration into the domain. We assume that Ω is closed and bounded.

To describe dispersal we denote $k_{ij}(x, y)$ as the probability that an individual at stage i which was produced from stage j at the point $y \in \Omega$ settles at $x \in \Omega$ during one dispersal period. Together, these kernels form the dispersal matrix $K(x, y) = (k_{ij}(x, y))$. The dispersal matrix may depend only on the signed distance $K(x, y) = K(x - y)$ rather than on precise locations, as is the case with the commonly used Laplace kernel with variance σ^2,

$$k(x, y) = \frac{1}{\sqrt{2\sigma^2}} \exp\left(-\sqrt{\frac{2}{\sigma^2}}|x - y|\right). \tag{4}$$

This kernel can be derived from the assumption that dispersers move randomly and settle at a constant rate [3,27]. If habitat quality, habitat selection, and boundary effects have to be taken into account [33], then the simplifying symmetry assumption is, in general, not valid. Dispersal kernels can also be constructed from observational data. If there is no mortality due to dispersal, then for all y

$$\int_\Omega k_{ij}(x, y)dx \le \int_{\mathbb{R}^n} k_{ij}(x, y)dx = 1, \tag{5}$$

since individuals are lost when they leave the domain. If there is mortality due to dispersal, then the second integral is less than one.

Now, for each stage i we multiply its production with its dispersal kernel, $k_{ij}b_{ij}u_j$, and sum over all stages j to obtain the spatially explicit model for reproduction and dispersal as (compare [26])

$$u(t + 1, x) = \mathcal{A}(u(t))(x) = \int_\Omega [K(x, y) \circ B(u(t, y), y)]u(t, y)dy, \tag{6}$$

where $\circ$ denotes the Hadamard product of entrywise matrix multiplication.

3.2. Analysis

Biologically, we are interested in finding the critical domain-size, its dependence on parameters, steady states and the long term behavior of solutions of (6). Mathematically, this translates into finding the leading eigenvalue of the linearization at zero, its dependence on parameters, bifurcations, and uniqueness and stability of fixed points. This section is devoted to provide all these mathematical tools.

The compactness and differentiability conditions established in Lemma 1 below ensure that we can use the theory of completely continuous operators in the analysis to follow. We then establish the main result on the linearization under quite strong assumptions (Theorem 1). In Section 3.2.2 we discuss how to relax these assumptions to include more biologically relevant scenarios. The proofs and some formulations in this section are quite technical and can be skipped at first.

Section 3.2.3 explores dependence on parameters. Lastly, we study existence and uniqueness of positive fixed points if the zero state is unstable.

It is convenient to work in the product space $\mathcal{L}^2 = (L^2(\Omega))^m$ and its positive cone. The following will be assumed throughout the paper.

(A1) The per capita production is bounded independent of the population size, i.e., $0 \le b_{ij}(u, y) \le b_{\max} < \infty$ for all i, j. Furthermore, $b_{ij}(u, y)$ is continuous w.r.t. y and continuously differentiable w.r.t. u.

(A2) If b_{ij} is nonzero then k_{ij} satisfies $k_{ij} \in (L^2(\Omega))^2$.

Lemma 1. *Under the assumptions (A1–2) it follows from Sections 17.3 and 17.8 in [21] that* $\mathcal{A} : \mathcal{L}^2 \to \mathcal{L}^2$ *as defined in (6) is positive and completely continuous. From Section 17.5 and Theorem 17.1 in [21] we see that* $\mathcal{A}$ *is strongly Fréchet differentiable at* $u = 0$ *w.r.t. the positive cone. Its derivative the positive, completely continuous linear operator given by*

$$\mathcal{A}'(0)\phi(x) = \mathcal{D}\phi(x) = \int_\Omega [K(x, y) \circ B(0, y)]\phi(y)dy. \tag{7}$$

Assumption (A1) generalizes [13,32] where it was assumed that the total production $f(u) = b(u)u$ is bounded independently of u. For a non-structured population, this assumption is natural. It implies that $b(u) \to 0$ as $u \to \infty$. This implication is too strong for the stage-structured model. In the scalar case, (A1) reduces to saying that f is asymptotically linear.

The "dispersal behavior" of sedentary stages is described by the delta distribution $k_{ij}(x, y) = \delta(x - y)$. This case is excluded by assumption (A2) since the operator $\mathcal{A}$ in general fails to be compact then. The last section of this paper is devoted to a more thorough investigation of this case.

3.2.1. Linear analysis

A linear operator is called *superpositive* [21] if it has a simple positive dominant eigenvalue with positive eigenfunction, and no other eigenfunction is positive. If an operator is superpositive then the stability of zero and the asymptotic behavior of the equation are determined by the leading eigenvalue and the corresponding eigenfunction. In what follows, we derive biologically relevant conditions under which $\mathcal{D}$ is superpositive.

A matrix B is called *primitive* if some power of B has strictly positive entries [6]. This condition is often satisfied in models for structured populations. We assume the following spatial version of primitivity.

(A3) The matrix $B(0, y)$ is primitive for each $y \in \Omega$ and its sign structure does not change throughout the domain, i.e., if $b_{ij}(0, y)$ is positive for some $y \in \Omega$ then it is positive for all $y \in \Omega$.

In biological terms, if stage j produces stage i somewhere in the domain, then it does so everywhere, possibly at different rates.

Theorem 1. *Assume (A1–3). In addition, assume that there are constants* $0 < \underline{\kappa} \le k_{ij} \le \overline{\kappa}$ *on* Ω *for all pairs* (i, j) *for which* b_{ij} *is nonzero. Then* $\mathcal{D}$ *is superpositive.*

We give the proof in appendix A.3 by first showing that the operator is u_0-positive in the sense of [20].

3.2.2. Relaxing the assumptions

The positivity assumption in Theorem 1 implies that dispersers can reach any point in the domain from any other point within one dispersal period. This assumption seems unreasonable for some species. In order to relax this assumption, we first assume the domain Ω to be connected. The condition on the kernels then becomes:

(A4) For all $k_{ij} \neq 0$ there is a simultaneous non-negative symmetric continuous subfunction $\kappa(x, y) = \kappa(y, x) \leq k_{ij}(x, y) \leq \overline{\kappa}$, and there is a constant δ such that for all $x \in \Omega$ the measure of the set $\{y \in \Omega \mid \kappa(x, y) \geq \underline{\kappa} > 0\}$ is at least δ.

The last condition in (A4) says that each point in the domain is accessible to individuals from an area of size at least δ. Assumption (A4) in particular covers two cases of interest. If dispersers stay close to where they originated then $k_{ij}(x, y) = 0$ if $|x - y|$ is large. The area from which a point can be reached then is a neighborhood of the point itself. In the other extreme, if individuals move at least a certain distance from where they originated, then the dispersal kernel is zero for $x = y$, as in the double Weibull kernel with appropriate parameters [27]. Then (A4) requires that the minimal distance which individuals travel is small enough compared to the domain size.

Proposition 1. *Assume (A1–4) and that Ω is connected. Then $\mathcal{D}$ is superpositive.*

Finally, we write $\Omega = \dot{\bigcup}_{\gamma=1\ldots\Gamma}\Omega_\gamma$ as a disjoint union of connected components. Hereafter, Latin characters always refer to stage whereas Greek characters refer to spatial domains. The *connectivity matrix* $C = (c_{\alpha\beta})$ for continuous kernels k_{ij} is given by

$$c_{\alpha\beta} = \begin{cases} 1 \text{ if for some} \quad x \in \Omega_\alpha, y \in \Omega_\beta, i, j : k_{ij}(x, y)b_{ij}(0, y) > 0 \\ 0 \text{ else} \end{cases} \tag{8}$$

Then we need the following last assumption

(A5) The matrix C is primitive.

Assumptions (A4) and (A5) together imply that an individual of stage i at point x can get to any other location $y \in \Omega$ and stage j through dispersal and production in finitely many generations. This assumption is the natural generalization of the assumption in [13] that dispersers can reach any point in the domain from any other point in finitely many generations. In mathematical terms this means that the operator $\mathcal{D}$ is irreducible.

Proposition 2. *Let $\Omega = \dot{\bigcup}_{\gamma=1\ldots\Gamma}\Omega_\gamma$ be the disjoint union of connected components and assume that (A1–5) hold. Then $\mathcal{D}$ is superpositive.*

Proofs of both propositions are given in appendix A.3.

3.2.3. *The relation between survival, growth and domain length*

We now study the dependence of the leading eigenvalue λ on some growth parameter P and on the domain length L.

Lemma 2. **(a)** *On a fixed domain, suppose that the matrix of production rates* $B(0, y; P)$ *is non-decreasing in* P. *Denote* $\lambda(P)$ *as the dominant eigenvalue. If at least one entry of* $B(0, y; P)$ *is strictly increasing in* P *then so is* $\lambda(P)$.

(b) *Fix* P, *and let* $\Omega = [0, L]$. *Assume that the kernel is of the form* $K(x, y) = K(x - y) > 0$ *and denote* $\lambda(L)$ *as the leading eigenvalue. Then* $\lambda(L)$ *is a strictly increasing function of* L.

Part (b) of the Lemma can be extended to higher dimensional domains and more general kernels. The formulation becomes more complicated, for example, one has to find an appropriate domain size parameter L. We formulate a more general version in appendix A.3 where we also give the proof.

The implicit function theorem applied at the bifurcation point gives

$$dP/dL < 0, \tag{9}$$

provided the conditions of the Lemma are satisfied. Hence, on smaller domains the population needs a higher growth rate to survive. This conclusion and inequality (9) were already reached in [32] for scalar integrodifference models. The correct proof, however, is provided in the two preceding lemmas.

3.2.4. *Nonlinear analysis*

To ensure existence of a nonzero fixed point, which is not the point at infinity, we impose the following condition.

(A6) There is some matrix-valued function $B(\infty, y)$ such that

$$\|B(u(y), y) - B(\infty, y)\| \leq \frac{\text{const.}}{\|u\|}, \qquad \text{for large} \quad \|u\|. \tag{10}$$

Lemma 3. *Suppose (A1,2,6) are satisfied. Then, by 3.2.1 in [20] and Theorem 17.2 in [21], the operator* $\mathcal{A}$ *has a strong asymptotic derivative at infinity. It is given by the completely continuous operator*

$$\mathcal{A}'(\infty)\phi(x) = \int [K(x, y) \circ B(\infty, y)]\phi(y)dy. \tag{11}$$

Proposition 3 (Existence of fixed points). *Assume (A1–6). Suppose that the spectral radius of* $\mathcal{A}'(\infty)$ *is less than one and that the dominant eigenvalue of* $\mathcal{D}$ *is greater than one. Then by Thm. 4.11 in [20],* $\mathcal{A}$ *has a positive fixed point. In the scalar case, the condition on the spectral radius at infinity reduces to the slant asymptote of* f *having slope less than one.*

(A7) The production rates satisfy $(\partial/\partial u_l)b_{ik} \leq 0$ for all i, k, l, and the inequality is strict for at least one set i, k, l.

Assumption (A7) states that the population experiences some population pressure. In particular, we exclude the *Allee effect* that a population benefits from an increase in density, at least for some intermediate density range. Recall that the dominant eigenvalue $\lambda(L, P)$ of the linear operator $\mathcal{D}(L, P)$ on $\Omega = [0, L]$ is increasing in the growth parameter P and the domain length L under some conditions. We first fix L and denote by $P^* = P^*(L)$ the critical value where $\lambda(L, P^*) = 1$.

Lemma 4 (Bifurcation I). *Assume (A1–7) are satisfied and the spectral radius of* $\mathcal{A}'(\infty)$ *is less than one, independent of* P *close to* P^*. *Assume that the production rates* b_{ij} *are non-decreasing in* P *and that at least one of the rates is increasing in* P. *Then there is a transcritical bifurcation at* $P = P^*$, *i.e., a continuous branch of solutions intersects the zero solution. The nonzero solution is positive for* $P > P^*$.

Vice versa, we can fix P and denote by $L^* = L^*(P)$ the critical domain length where $\lambda(L^*, P) = 1$. To formulate the next lemma, it is convenient to introduce the *dispersal success functions*

$$s_{ij}(y) = \int_{\Omega} k_{ij}(x, y)dx, \tag{12}$$

which we discuss in detail in Section 5.

Lemma 5 (Bifurcation II). *Assume (A1–7) are satisfied and the spectral radius of* $\mathcal{A}'(\infty)$ *is less than one, independent of* L *close to* L^*. *Assume that the dispersal success functions* s_{ij} *are non-decreasing in* L *and that at least one of them is increasing in* L. *Then there is a transcritical bifurcation at* $L = L^*$, *i.e., a continuous branch of solutions intersects the zero solution. The nonzero solution is positive for* $L > L^*$.

The proofs are given in appendix A.3.

In the scalar case it is known [32] that the non-negative fixed point is unique and stable whenever it exists, provided that the function $f(u) = b(u)u$ is monotone and concave. The Beverton-Holt growth function satisfies the conditions but the Ricker function does not. The result can be generalized to the stage-structured model as follows.

Proposition 4 (Uniqueness of fixed points). *Let the assumptions of Proposition 3 be satisfied. Assume in addition that the function*

$$u \mapsto B(u)u \tag{13}$$

is increasing and that

$$t \mapsto B(tu) \tag{14}$$

is decreasing for $0 \le t \le 1$. *Then* $\mathcal{A}$ *is concave and monotone and hence by Thm. 6.3 in [20] the positive fixed point is unique. By Thm. 6.6 in [20] every solution with* $u_0 \neq 0$ *converges to the positive fixed point.*

In appendix A.2, conditions (13), (14) are given in coordinates and some examples that satisfy the two conditions are worked out. In natural populations, periodic cycles occur frequently and hence a unique stable fixed point may be unrealistic.

4. Example and simulations

We introduce dispersal into the matrix model from [25] on a connected one-dimensional habitat patch. Simulations illustrate the theory above. In particular, we ask: Keeping the dispersal parameters fixed, how does the behavior of the spatial model compare to the one of the non-spatial model? Vice versa, keeping the population vital rates fixed, how does the behavior of the spatial model depend on dispersal?

The population in the matrix model [25] is divided into juveniles, u_1, and adults, u_2. Survival of stage j is given by the rate ρ_j. Juveniles mature at rate γ, and adults produce juveniles at rate P. The model equation reads

$$u(t+1) = Bu(t) = \begin{pmatrix} \rho_1(1-\gamma) & P \\ \rho_1\gamma & \rho_2 \end{pmatrix} u(t), \qquad u = \begin{pmatrix} u_1 \\ u_2 \end{pmatrix}. \tag{15}$$

In [25], a detailed study is given in the four cases that exactly one of the parameters depends on the total density $u_1 + u_2$ according to a negative exponential. We concentrate on the case of density-dependent reproduction, i.e., we replace the parameter P in (15) by $Pe^{-(u_1+u_2)}$. The results from [25] in that case are: For small values $P < P_0$ the zero state is the unique stable equilibrium of (15). At $P = P_0$ there is a transcritical bifurcation to a stable positive equilibrium. For $P > P_c$ this equilibrium loses stability through a series of flip bifurcations, which eventually lead to chaotic behavior ([25], Figures 2a, 5a). The bifurcation values P_0 and P_c as well as the population level at the positive steady state and the basic reproductive number R_0 are computed explicitly ([25], Equation (9) and Tables 3, 4).

We choose each dispersal kernel as a Laplace kernel and, for simplicity, assume that all kernels have the same variance, i.e., $k_{ij}(x, y) = k(x, y)$ as in (4). We work on the normalized spatial domain $\Omega = [-1, 1]$. Changing the domain to $[-L, L]$ is equivalent to replacing the variance of the kernels by σ^2/L^2, [32]. Instead of P and L we work with P and σ^2.

The assumptions of Theorem 1 and Lemma 2 are satisfied. Therefore, there is a leading eigenvalue, and it is increasing in P and L, and hence decreasing in σ^2. Assumption (A6) is satisfied with

$$B(\infty) = \begin{pmatrix} \rho_1(1-\gamma) & 0 \\ \rho_1\gamma & \rho_2 \end{pmatrix}. \tag{16}$$

Hence, by Proposition 3 there is a fixed point in case that the leading eigenvalue of the linearization is greater than 1. There is no Allee effect, and hence by Lemmas 4 and 5 there are transcritical bifurcations from the trivial steady state as P increases or σ^2 decreases.

Since we are interested in the effects of space, we concentrate on σ^2 and fix the other parameters as in [25], i.e., $\rho_1 = 0.5$, $\rho_2 = \gamma = 0.1$. Figure 1 shows, for fixed P, how the stable equilibrium emerges and changes shape for decreasing variance σ^2 (or increasing domain length L). Both, juveniles and adults, grow with the domain length. The dashed lines give the dispersal success approximation as explained in Section 5. Simulations are done using MATLAB, its FFT-routine and 4096 space points.

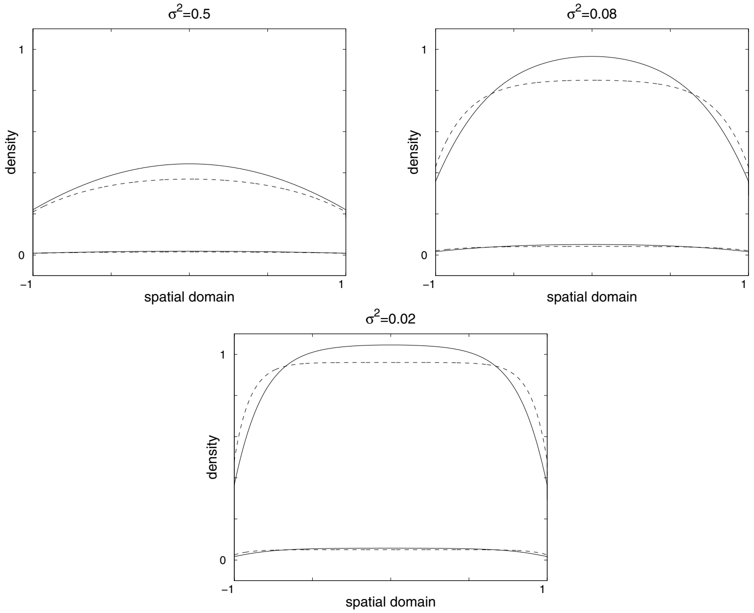

Fig. 1. The true steady state (solid line) and the dispersal success approximation (dashed line) for $P = 30$ and $\sigma^2 = 0.5$, $\sigma^2 = 0.08$ and $\sigma^2 = 0.02$. The upper profiles show the juveniles, the lower ones the adults.

The exponential density-dependence $Pe^{-(u_1+u_2)}$ does not satisfy the concavity condition (13) for uniqueness of fixed points in Proposition 4. Hence, we expect further bifurcations for appropriately chosen values of P. All density profiles in Figure 1 are concave, which simply is an effect of the loss of individuals through the boundary. It turns out that secondary bifurcations, domain length and non-concave profiles are closely related.

In Figure 2 we give some examples of cycles with non-concave shapes. The two local maxima near the edges of the domain in the 2-cycle result from an interplay of loss through the boundary, the Ricker dynamics and the small (relative to the domain size) dispersal distance. If the population density at the boundary is lower than in the middle of the domain, then the Ricker dynamics produce more individuals close to the boundary than in the middle. Since dispersal is small, this pattern is still seen after the smoothing effect of dispersal. In the next time step, the Ricker dynamics produce only few offspring close to the boundary, some of which are then lost through the boundary, and hence we are back to the beginning.

Since all the dispersal kernels are equal, we can explicitly compute the relationship between the intrinsic growth rate and the domain length at the first bifurcation point, thereby extending the results in [19,32]. We denote $\phi = (\phi_1, \phi_2)$ and write the linearized equation as

$$\lambda\phi(x) = \int_{-1}^{1} \frac{1}{\sqrt{2\sigma^2}} \exp\left(-\frac{|x-y|}{\sqrt{\sigma^2/2}}\right) B\phi(y)dy, \tag{17}$$

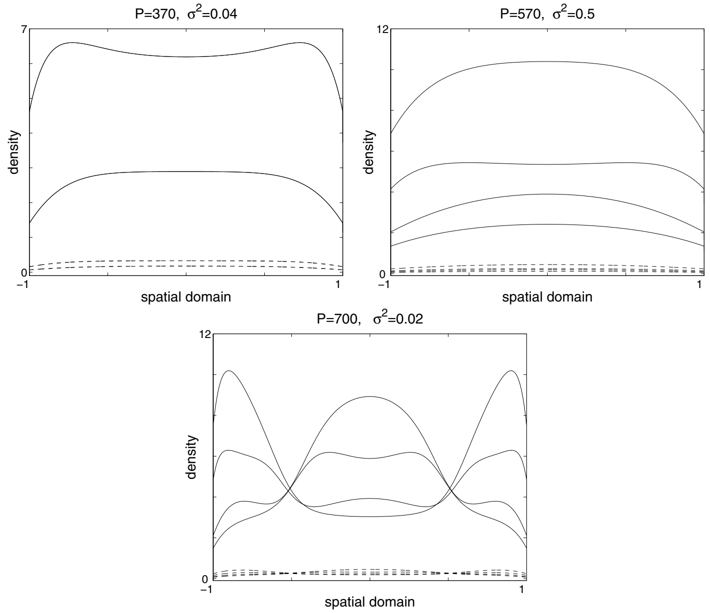

Fig. 2. Non-concave shapes of cycles. The 2-cycle for $P = 370$ and $\sigma^2 = 0.08$ shows one non-concave profiles for juveniles (solid lines). Similarly, the 4-cycle for $P = 570$ and $\sigma^2 = 0.5$. The last plot shows a 4-cycle for $P = 700$ and $\sigma^2 = 0.02$, in which also the adult stage has non-concave profiles.

with B as in (15). Differentiating twice leads to the equivalent formulation

$$\phi''(x) = -\sqrt{\frac{2}{\sigma^2}}\left(\frac{1}{\lambda}B - I\right)\phi(x), \tag{18}$$

with boundary conditions

$$\phi'(\pm 1) \pm \sqrt{\frac{2}{\sigma^2}}\phi(\pm 1) = 0. \tag{19}$$

At the bifurcation point, we have $\lambda = 1$, which implies that the leading eigenvalues of B is greater than 1. Solutions of the boundary value problem (18), (19) are symmetric with respect to $x \longmapsto -x$. The exponential ansatz $\phi(x) = \psi e^{\zeta x}$ leads to

$$\zeta^2 = -\sqrt{\frac{2}{\sigma^2}}(\mu_j - 1), \tag{20}$$

where $\mu_{1,2}$ are the eigenvalues of B with the corresponding eigenvectors $\psi_{1,2}$. We have $\mu_1 > 1$, $\mu_2 < 1$. Applying the symmetry condition, we are left with the two possible solutions

$$\psi_1 \cos\left(\frac{\sqrt{\mu_1 - 1}}{\sqrt{\sigma^2/2}}x\right), \qquad \psi_2 \cosh\left(\frac{\sqrt{1 - \mu_2}}{\sqrt{\sigma^2/2}}x\right). \tag{21}$$

Using the boundary conditions and the requirement that the solution be positive, we can rule out the second possibility and arrive at the relation

$$\sqrt{\frac{2}{\sigma^2}} = \frac{\tan^{-1}(1/\sqrt{\mu_1 - 1})}{\sqrt{\mu_1 - 1}}, \tag{22}$$

which for the scalar case was given in [19] equation (60), and [32] equation (28). This argument generalizes to arbitrary dimension provided that all eigenvalues of B are real and only the leading eigenvalue is greater than 1.

The leading eigenvalue μ_1 of B obviously depends on the growth parameter P. We plot the relation between σ^2 and P in Figure 5, where we compare it with approximative values derived in Section 5 and results from numerical experiments.

5. Approximations

Dispersal matrices contain many parameters, and model (6) might require intensive computing. In this section, we present some helpful approximations. These approximations are based on the *redistribution function*, the *dispersal success function*, and the *average dispersal success* which we introduce below. The *patch approximation* reduces the integrodifference equation to a difference equation in some finite dimensional state space. It was first mentioned in [13] for a non-structured population. The *dispersal success approximation* gives the approximate spatial distribution of the stationary solution of the integrodifference equation in terms of the stationary solution of the non-spatial model and some information about the dispersal process. It was first worked out for a non-structured population on a single habitat patch in [32] and for two patches in [14]. The underlying idea for both approximations is to average over homogeneous habitat-patches. We generalize both approximations to a stage-structured population on finitely many habitat-patches. Then we derive approximations of the eigenvalues which determine persistence and stability of a population.

5.1. Characteristics of dispersal

Integrating the dispersal kernels with respect to point of settlement, we obtain the *dispersal success functions* $s_{ij}(y)$. These give the probability with which an individual of stage i that was produced from stage j at location y after the dispersal phase successfully settled in the domain Ω. The matrix of dispersal success functions is defined by

$$S(y) = \int_\Omega K(x,y)dx = \left(\int_\Omega k_{ij}(x,y)dx\right) = (s_{ij}(y)). \tag{23}$$

If no individuals are lost through the boundary then $s_{ij}(y) = 1$ (compare (5)) but in general

$$0 \le s_{ij}(y) \le 1. \tag{24}$$

The functions $s_{ij}(y)$ correspond to a point release experiment. At the point y one releases individuals of stage i produced from stage j, and after one dispersal period one determines the fraction of individuals that are still in the domain. The *average dispersal success* is given by

$$\hat{S} = \frac{1}{|\Omega|}\int_\Omega S(y)dy = \frac{1}{|\Omega|}\int_\Omega\int_\Omega K(x,y)dydx. \tag{25}$$

The *redistribution functions* $r_{ij}(x)$ correspond to an area release experiment. Individuals of stage i produced from stage j are distributed homogeneously over the whole domain with density N. After one dispersal period the expected density of individuals at $x \in \Omega$ is $Nr_{ij}(x)$. The matrix of redistribution functions is

$$R(x) = \int_\Omega K(x,y)dy = \left(\int_\Omega k_{ij}(x,y)dy\right) = (r_{ij}(x)). \tag{26}$$

The function R is nonnegative but need not be bounded pointwise.

If the probability of dispersing from y to x is the same as the one from x to y, the dispersal kernel is symmetric, $K(x,y) = K(y,x)$, which implies $R = S$. The Laplace kernel (4) is an example. Its dispersal success function is given by

$$s(y) = 1 - \frac{1}{2}e^{-\sqrt{\frac{2}{\sigma^2}}}\cosh\sqrt{\frac{2}{\sigma^2}}y, \tag{27}$$

see [32], and the average dispersal success is (see Figure 3)

$$\hat{s} = 1 - \frac{1}{2}\sqrt{\frac{\sigma^2}{2}}\left(1 - e^{-2\sqrt{\frac{\sigma^2}{2}}}\right). \tag{28}$$

In general, the two functions R and S are different. Assume, for example, that in a non-structured population ($m = 1$) the choice of settlement location depends only on the quality of the habitat at that point. Then $k(x,y) = k(x)$, and so the redistribution function $r(x)$ is just a multiple of k whereas the dispersal success function $s(y)$ is constant.

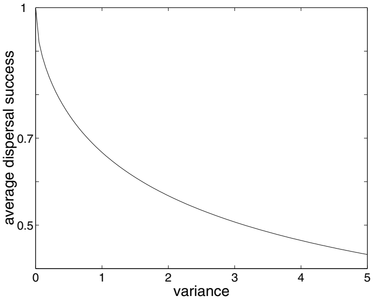

Fig. 3. The average dispersal success $\hat{s}$ of the Laplace kernel (4) depending on the variance σ^2.

5.2. Patch approximation

We assume that Ω is divided into disjoint connected components Ω_α, $\alpha = 1 \dots \Gamma$, each of which is spatially homogeneous. Recall that Greek letters to refer to space and Latin ones to stage. Averaging the population over each component, we get the vectors $U^\alpha(t) = (U_1^\alpha(t), \dots, U_m^\alpha(t))^T$ as

$$U^\alpha(t) = \frac{1}{|\Omega_\alpha|} \int_{\Omega_\alpha} u(t,x)dx \tag{29}$$

for each patch Ω_α. On each patch we get the matrix of production rates

$$B^\alpha(\cdot) = B(\cdot, y)_{|\Omega_\alpha}. \tag{30}$$

Substituting (29) and (30) into the right hand side of the master equation (6) and integrating the result over habitat patch α we obtain the time evolution of the population averages as the $m \times \Gamma$-dimensional system

$$U^\alpha(t+1) = \sum_{\beta=1}^{\Gamma} \left[S^{\alpha\beta} \circ B^\beta(U^\beta(t)) \right] U^\beta(t), \tag{31}$$

where $S^{\alpha\beta}$ are matrices of averaged dispersal success from patch Ω_β to Ω_α,

$$S^{\alpha\beta} = \frac{1}{|\Omega_\alpha|} \int_{\Omega_\alpha} \int_{\Omega_\beta} K(x,y)dydx, \qquad \alpha, \beta = 1, \dots, \Gamma. \tag{32}$$

On a single patch, formula (31) simplifies to an equation of the form (2):

$$U(t+1) = [\hat{S} \circ B(U(t))]U(t), \tag{33}$$

where $\hat{S}$ is the average dispersal success given by (25).

Since the integration over space has to be performed only once instead of at every time step, the iteration (31) is computationally faster than the full model (6), in particular, if the integrals are not convolutions. If dispersal is homogeneous within patches then the approximation (31) is indeed the true solution of (6).

5.3. Dispersal success approximation

We briefly recall the approximation for an unstructured population and a symmetric kernel as derived in [32]. Denote $u^*(x)$ as the nonzero equilibrium solution of (3) and $\bar{u}$ as its spatial average. If $|u^*(x) - \bar{u}|$ is small, then the dispersal success approximation

$$u^*(x) = s(x)b(\bar{u}_a)\bar{u}_a, \tag{34}$$

is of first order in $|u^*(x) - \bar{u}|$. Integrating this equation on both sides gives the spatial average $\bar{u}$ as the approximate solution of the algebraic equation

$$\bar{u}_a = \hat{s}b(\bar{u}_a)\bar{u}_a, \tag{35}$$

where $s(x)$ and $\hat{s}$ are given by (23) and (25). The corresponding formula in the case of two habitat-patches has been derived in [14]. Dropping the assumption of symmetric kernels, we instead get the *redistribution approximation*

$$u^*(x) = r(x)b(\bar{u}_a)\bar{u}_a, \tag{36}$$

where $r(x)$ is the redistribution function (26) for the kernel k and $\bar{u}_a$ is still given by (35). Recall that (34) and (36) can be quite different.

In the stage-structured case on a single habitat-patch Ω, we denote by u^* the stationary solution of (6) and form the average

$$\bar{u} = (\bar{u}_1, \dots, \bar{u}_m)^T = \frac{1}{|\Omega|}\int_\Omega u^*(x)dx. \tag{37}$$

We abbreviate $\mathcal{F}(w) = [K \circ B(w)]w$. Using the fundamental theorem of calculus, the steady state equation of (6) can be written as

$$\begin{aligned} u^*(x) = &\int_\Omega [K(x, y) \circ B(\bar{u}, y)]dy\,\bar{u} \\ &+ \int_\Omega \int_0^1 D\mathcal{F}(\xi u^* + (1-\xi)\bar{u})\,d\xi\,(u^* - \bar{u})\,dy, \end{aligned} \tag{38}$$

where $D\mathcal{F}$ denotes the derivative of $\mathcal{F}$. We now assume that the steady state solution u^* is close to its spatial average and that $D\mathcal{F}$ is order 1. These assumptions are valid if the domain is large with respect to the dispersal distance and if the production rates are smooth functions of the density. We also assume that the habitat is homogeneous such that B does not depend on y. Then to first order we have

$$u^*(x) = \left[\int_\Omega K(x, y)dy \circ B(\bar{u})\right]\bar{u} = [R(x) \circ B(\bar{u})]\bar{u}, \tag{39}$$

and in the special case of symmetric kernels $u^*(x) = [S(x) \circ B(\bar{u})]\bar{u}$. Integrating both sides and dividing by the volume of Ω, we get the vector-valued fixed-point equation

$$\bar{u}_a = [\hat{S} \circ B(\bar{u}_a)]\bar{u}_a, \tag{40}$$

with $\hat{S}$ as in (25), which determines $\bar{u}$ to first order.

For several homogeneous habitat patches Ω_α, $\alpha = 1 \dots \Gamma$, with $B^\alpha(\cdot) = B(\cdot, y)_{|\Omega_\alpha}$, the redistribution approximation is given by

$$u^*(x) = \sum_\alpha [R^\alpha(x) \circ B^\alpha(\bar{u}^\alpha)]\bar{u}^\alpha, \tag{41}$$

where $R^\alpha(x)$ is the number of arrivals at x from patch Ω_α. For symmetric kernels we obtain the dispersal success approximation by replacing R^α with S^α, where $S^\alpha(x)$ is the dispersal success from x into patch Ω_α, compare (32). The first-order approximation of the population average at the equlilbrium solution is given by the fixed point of the matrix-valued equation

$$\bar{u}^\alpha = \sum_\beta [S^{\alpha\beta} \circ B^\beta(\bar{u}^\beta)]\bar{u}^\beta. \tag{42}$$

5.4. Example continued

Since all dispersal kernels in our example are assumed identical, the dispersal success approximation of the spatial version of (15) simplifies to

$$u^*(x) = s(x)B(\bar{u})\bar{u}, \qquad \bar{u}_a = \hat{s}b(\bar{u}_a)\bar{u}_a. \tag{43}$$

The result is plotted as the dashed lines in Figure 1. True and approximation solution agree well for the adult stage but not quite as well for the juvenile stage. In deriving the dispersal success approximation, we assumed that the profile is sufficiently close to a constant. Whereas the adult stage is close to a constant, the juvenile stage is not, and hence the difference was to be expected.

5.5. Eigenvalue approximation

We now approximate the leading eigenvalue λ of the operator $\mathcal{D}$ in (7). We denote the corresponding eigenfunction by $\phi = (\phi_1, \ldots, \phi_m)^T$. On each patch Ω_α we get the average $\bar{\phi}^\alpha$ as in (29). Assuming again that B is constant on each patch Ω_α, we integrate both sides of the equation $\lambda\phi = \mathcal{D}\phi$ over the domain and substitute $\bar{\phi}$ for ϕ to get the approximate equation

$$\lambda\bar{\phi}_\alpha = \sum_\beta \left[S^{\alpha\beta} \circ B^\beta(0)dy\right]\bar{\phi}_\beta, \tag{44}$$

with $S^{\alpha\beta}$ as in (32). On a single habitat patch the formula is

$$\lambda\bar{\phi} = \left[\hat{S} \circ B(0)\right]\bar{\phi}, \tag{45}$$

which is exactly the eigenvalue problem for (33) linearized at zero.

Since individuals may be lost through the boundary, one expects that the total number of individuals at steady state in the spatial model (6) is lower than in the non-spatial model (2). Also, one expects that the leading eigenvalue of the linearization in the spatial case is smaller than the one for the corresponding non-spatial model, i.e., in the spatial case, the population needs to have a higher growth rate in order to persist. The following lemma can be shown using the theory of positive operators [20].

Lemma 6. *Denote by λ_n the leading eigenvalue of the linearization $\phi \mapsto B(0)\phi$ of the non-spatial model (2) and by λ_{sp} the leading eigenvalue of the approximation of the linearized spatial model (45). Then*

$$\lambda_{sp} \le \lambda_n.$$

Next, assume that both models (2) and (6) have a unique positive fixed point. Denote by $\hat{u} = F(\hat{u}) = B(\hat{u})\hat{u}$ the fixed point of the non-spatial model and by $\bar{u}_a$ the fixed point of the approximation of the spatial model, see (40). In the case of only one stage ($m = 1$) assume that $F'(\bar{u}_a) < 1$. In the general case assume that F is monotone and asymptotically sublinear. Then

$$\bar{u}_a \le \hat{u}.$$

Finally, we find appoximate conditions for stability of the positive steady state. We denote $u^*(x)$ and $\bar{u}$ as above, and start with an unstructured population on a connected habitat. Then, for some function $w(t,x)$ close to u_*, the difference satisfies

$$\begin{aligned} &w(t+1,x) - u^*(x) \\ &\quad = \int k(x,y)[f(w(t,y)) - f(\bar{u})]dy + \int k(x,y)[f(\bar{u}) - f(u^*(y))]dy \\ &\quad \approx \int k(x,y) f'(\bar{u})[w(t,y) - u^*(y)]dy. \end{aligned}$$

An approximation of the eigenvalue at the steady state of (3) is hence given by the eigenvalue equation

$$\lambda\phi = f'(\bar{u}) \int k(x,y)\phi(y)dy = (b(\bar{u}) + b'(\bar{u})\bar{u}) \int k(x,y)\phi(y)dy, \qquad (46)$$

which has a simple dominant real eigenvalue of the same sign as $f'(\bar{u})$ and in absolute value less than $f'(\bar{u})$. Replacing ϕ by its spatial average gives an approximation in terms of the average dispersal success,

$$\lambda \approx \hat{s} f'(\bar{u}) = \hat{s}(b(\bar{u}) + b'(\bar{u})\bar{u}). \qquad (47)$$

For $m > 1$ stages the eigenvalue of the steady state $u_*(x)$ is approximated by the eigenvalue equation (compare [6] for the non-spatial case)

$$\lambda\bar{\phi} = [\hat{S} \circ B(\bar{u})]\bar{\phi} + \sum_1^m \left[\hat{S} \circ \frac{\partial B(\bar{u})}{\partial u_k} \bar{u} \right] \bar{\phi}_k. \qquad (48)$$

5.6. Example continued

The approximate linearized model is $\phi \mapsto \hat{s}B(0)\phi$. Hence, its leading eigenvalue $\lambda_{sp} = \hat{s}\lambda_n$ is just a multiple of the eigenvalue of the non-spatial model with $\hat{s} \leq 1$. This was the first claim of Lemma 6. For the second claim, we denote $\bar{u}(\hat{s})$ as the fixed point in (43) and $\hat{u}$ as the fixed point of the non-spatial model (15). Obviously, $\bar{u}(1) = \hat{u}$. Both components of $\bar{u}$ are increasing functions of $\hat{s}$, as plotted in Figure 4, and hence, $\bar{u} \leq \hat{u}$.

Following [25], we can compute the first bifurcation point $P_0(\hat{s})$ of (43),

$$P_0(\hat{s}) = \frac{(1 - \hat{s}\rho_2)(1 - \hat{s}\rho_1(1-\gamma))}{\hat{s}^2 \rho_2 \gamma}. \qquad (49)$$

The point at which the positive steady state loses stability is given by

$$P_c(\hat{s}) = P_0(\hat{s}) \exp\left\{ \frac{2\hat{s}(1 - \hat{s}\rho_2 + \hat{s}\rho_1\gamma)(\rho_1(1-\gamma) + \rho_2)}{(1 + \hat{s}\rho_2 - \hat{s}\rho_1\gamma)(1 - \hat{s}\rho_2)(1 - \hat{s}\rho_1(1-\gamma))} \right\}. \qquad (50)$$

These two bifurcation points are approximations to the bifurcations of the spatially explicit model according to the eigenvalue approximations (45) and (48).

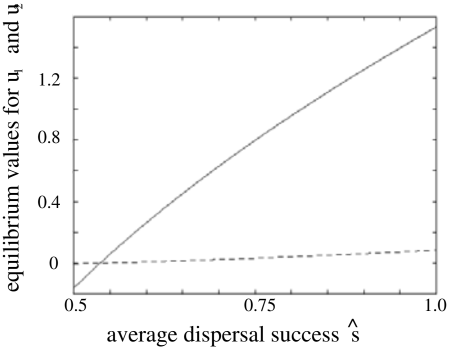

Fig. 4. The equilibrium $\bar{u}_1$ (solid) and $\bar{u}_2$ (dashed) as a function of $\hat{s}$.

In Figure 5 we plot P_0 and P_c as functions of the variance σ^2. We see that P_0 is a good approximation to the true value given by (22). We also plot the results of some numerical experiments done on the spatially explicit model. The bifurcation points predicted by the approximation and the results from the numerical experiment agree quite well. The secondary bifurcation point P_c is decreasing for very small variances. This fact is somewhat surprising since dispersal in space usually

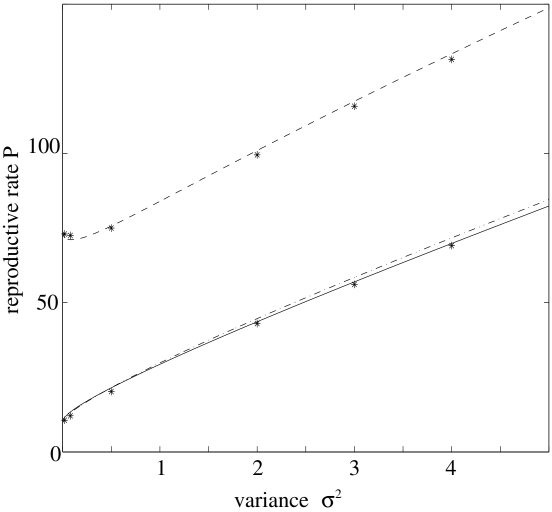

Fig. 5. True, approximate and experimental relation between P and σ^2 at the first and second bifurcation point. The true relation at the first bifurcation as given by formula (22) is plotted as the dash-dot line. It agrees quite well with the function P_0 (solid) from the approximation (49) and with the bifurcation values found in numerical experiments (stars). The relation at the second bifurcation point cannot be computed explicitly. The approximation P_c (dashed) as in (50) agrees quite well with the experimental values (stars).

has a stabilizing effect. But the numerical results are independent of the number of grid points, and the first order approximation shows the same behavior.

6. Application

We study the simplest occurence of habitat fragmentation, namely how a gap in the domain affects population persistence and dynamics. More specifically, we show how the population is affected by a disturbance of fixed size, depending on where the disturbance occurs. This investigation is by no means complete since the number of parameters increases dramatically as we add space and dispersal to matrix models. But it shows how the tools developed above can be applied to real ecosystems.

We continue the example from Section 4 on the domain $[-1, 1]$, from which we delete a connected subdomain of length 0.1, i.e., 5% of the total domain. Hence, the total domain consists of two patches

$$\Omega = [-1, M - 0.05] \cup [M + 0.05, 1], \tag{51}$$

where M denotes the center of the gap. Since the dispersal kernel is symmetric, it suffices to look at $0 \leq M \leq 0.95$.

First, we study how persistence of the population is affected depending on which part of the domain is missing. In Figure 6 we plot the maximum densities of u_1 and u_2 and the approximate eigenvalue (45) as a function of M. The parameters are $P = 15$ and $\sigma^2 = 0.08$. We see that the population does not survive if the gap is in the middle of the domain, but it is established if the gap is closer to the boundary of the domain. According to the nonlinear model, the critical value is $M \approx 0.15$. The approximate eigenvalue at $M = 0.015$ is $\lambda_n \approx 0.99$ and hence, the approximation is within 1% of the true value.

Next, we show that for different parameters, $P = 82, \sigma^2 = 0.5$ a population might or might not exhibit cycles, depending on where the gap is in the domain. Figure 7 shows the two extreme cases with the gap being in the middle and the population at a stable steady state (left) and the case without gap and the population

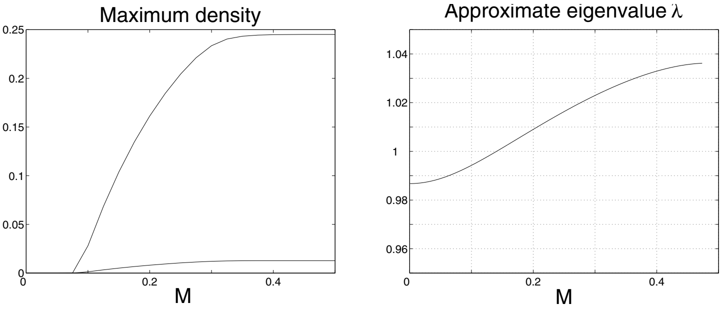

Fig. 6. Persistence and gap location. The maximum density of u_1 and u_2 shows a transcritical bifurcation as the center point of the gap, M, is shifted from the center of the domain ($M = 0$) to the boundary ($M = 0.95$). On the right, the approximate eigenvalue is plotted.

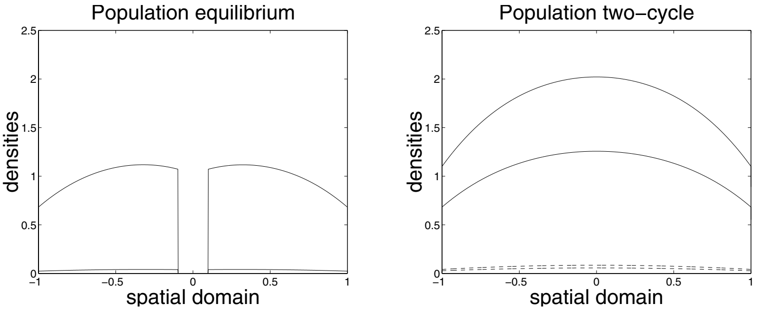

Fig. 7. Dynamics and gap location. With the gap in the middle, the population reaches a stable steady state (left). Without gap, the population exhibits a two-cycle (right). The solid lines represent u_1, the dashed lines are u_2.

exhibiting a two-cycle (right). As the gap is moved outwards from the center, the amplitude of the cycles decreases until the cycles disappear at some point.

7. Stages without dispersal

Not always do individuals move between two successive reproductive phases. Mathematically, this "staying-in-place" strategy [12] is described by the kernel $k(x, y) = \delta(x - y)$. In assumption (A2) we excluded this choice of k since the operator $\mathcal{A}$ in (6) would not be compact. This problem was already mentioned in [13], where, in order to make the theory applicable, the delta distribution was replaced by some approximate kernel which insured the necessary compactness properties.

In the study of speeds and shapes of traveling fronts, compactness of the operator $\mathcal{A}$ is not required. For a single population, in which some proportion is not dispersing, the speed of the front was studied in [34]. For structured populations the speed of a front was given in [26].

Sedentary stages occur naturally in structured populations. In many cases, the theory developed in Section 3 can still be applied. The biological reason for this is that wherever one starts in the life cycle, one has to go through some dispersal phase eventually. Mathematically, this means we look at some power $\mathcal{A}^n$ of the operator $\mathcal{A}$.

As an example, we first consider a biannual species, in which both age classes reproduce. The matrix B is the simplest primitive Leslie matrix

$$B = \begin{pmatrix} \beta_1 & \beta_2 \\ \mu & 0 \end{pmatrix}, \tag{52}$$

where β_j is the production rate from stage j and μ is the survivorship. If we assume that dispersal occurs only at reproduction, then $k_{21} = k_{22} = \delta$. We denote $k_{11} = k_1$, $k_{12} = k_2$. Then

$$\begin{aligned} u_1(t+1, x) &= \int k_1(x, y)\beta_1(u(t, y))u_1(t, y) + k_2(x, y)\beta_2(u(t, y))u_2(t, y)dy, \\ u_2(t+1, x) &= \mu u_1(t, x). \end{aligned} \tag{53}$$

The operator $\mathcal{A}$ here is not compact. However, the operator $\mathcal{A}^2$ given by

$$\begin{aligned} u_1(t+2,x) &= \int k_1(x,y)\beta_1(u(t+1))u_1(t+1,y)dy \\ &\quad + \int k_2(x,y)\beta_2(u(t))\mu u_1(t,y)dy, \\ u_2(t+2,x) &= \mu \int k_1(x,y)\beta_1(u(t,y))u_1(t,y) \\ &\quad + k_2(x,y)\beta_2(u(t,y))u_2(t,y)dy, \end{aligned} \tag{54}$$

is compact as long as $\mu > 0$ is independent of u. Hence, the theory developed in Section 3 applies to $\mathcal{A}^2$.

To proceed with the general theory we first consider the linear case, in particular the study of critical domain-size for the case with sedentary stages. We restrict ourselves to the case of a connected habitat Ω. We decompose the linear operator (7)

$$\mathcal{D}\phi(x) = \int [K(x,y) \circ B(0,y)]\phi(y)dy = (\mathcal{D}_1 + \mathcal{D}_2)\phi(x), \tag{55}$$

such that $\mathcal{D}_1$ contains all the entries where k_{ij} satisfies (A2) and is zero otherwise. The operator $\mathcal{D}_2$ contains the functions b_{ij} where $k_{ij} = \delta$ and is zero otherwise. Then $\mathcal{D}_1$ is compact and $\mathcal{D}_2$ is bounded. The following lemma is proved in appendix A.3.

Lemma 7. *Assume that $\mathcal{D}_2$ is nilpotent of order n_0, uniformly in $y \in \Omega$. Then $\mathcal{D}^n$ is compact for all $n \geq n_0$. If, in addition, assumptions (A1,3) hold and (A4) holds for the kernels in $\mathcal{D}_1$, then $\mathcal{D}$ is superpositive for some $n \geq n_0$. In particular, if the spectral radius of $\mathcal{D}$ is greater than one, then the zero solution of (6) is unstable.*

The conditions in the nonlinear case are somewhat more restrictive. We now decompose the nonlinear operator (6)

$$\mathcal{A}(u)(x) = \int K(x,y) \circ B(u(y),y)u(y)dy = (\mathcal{A}_1(u) + \mathcal{A}_2(u))(x) \tag{56}$$

as above, i.e., such that $\mathcal{A}_1$ contains all the entries where k_{ij} satisfies (A2) and is zero otherwise. The operator $\mathcal{A}_2$ contains the functions b_{ij} where $k_{ij} = \delta$ and is zero otherwise. Then $\mathcal{A}_1$ is compact and $\mathcal{A}_2$ is bounded.

Lemma 8. *Assume that $\mathcal{A}_2$ is linear in u and nilpotent of order n, uniformly in $y \in \Omega$. Then $\mathcal{A}^n$ is completely continuous.*

If the assumptions of the previous lemma are satisfied, then existence of fixed points for $\mathcal{A}^n$ can be studied as in Proposition 3. A fixed point of $\mathcal{A}^n$, of course, corresponds to a periodic orbit of $\mathcal{A}$, such that the period is a divisor of n. However, the operator $\mathcal{A}^{n+1}$ is likewise compact. If for both powers, n and $n+1$ existence of a unique fixed point can be established, then this fixed point is also the unique fixed point for $\mathcal{A}$.

To conclude, we discuss two examples. Structuring a population by age, one obtains a Leslie matrix for B [23]. If dispersal occurs during reproduction, then the conditions of the previous lemma are satisfied. Grouping individuals by some stage other than age, generally gives a positive probability that an individual stays in the same age class for more than one time step. If the stages are ordered successively then B has the form of a Lefkovitch matrix [22], which is a Leslie matrix with additional terms on the diagonal. In that case, all the kernels on the diagonal must satisfy (A2), i.e., individuals which remain in some age class must disperse, in order for the assumption of the previous lemma to be satisfied. However, this seems to be an artifact of the grouping. If one assumes that for each state there is a maximum number of cycles for which an individual can remain in this stage, then dividing each state into the maximal number of cycles within that stage, one obtains a matrix B on a larger state space but with no diagonal entries. Hence, assuming dispersal only during reproduction is again sufficient to satisfy the assumptions of the previous lemma.

8. Discussion

Analysis of the critical domain-size problem is a crucial aspect of the mathematics of conservation. Stage-structured matrix models are well established as models for populations at risk [6], but do not include explicit spatial aspects of the species' habitat and dispersal. In this paper, we include these aspects into matrix models and analyze persistence and bifurcation of solutions to the resulting matrix integrodifference equations.

The strength of such stage-structured integrodifference models is that they allow explicit depiction of specific life stages and dispersal events. Although the full model formulation is complex, various approximations allow us to simplify the explicit spatial model into a pseudo-spatial matrix model. These are the dispersal success approximation and the redistribution approximation. From these we can approximate the spatial solutions and their bifurcation structure.

This work can be considered as an extension of Van Kirk and Lewis' [32] analysis of scalar integrodifference models to include stage-structure, fragmented habitats, and non-dispersing stages. The results in Section 3 are similar to their results for non-structured populations in connected habitats. The technical issues of compactness of the operator when there are non-dispersing stages are not fully resolved (Section 7), although, for typical models, the operator can be shown to be compact by analyzing population dynamics over an extended time step.

In Theorem 1 and its generalizations, we list sufficient conditions for the theory to work, mainly compactness, positivity and irreducibility. In case compactness fails, Section 7 gave conditions under which the results still apply. If irreducibility fails, for example if (A3) is violated, then the eigenvalue need not be simple and the components of the eigenfunction need not all be positive. Note that irreducibility requires an interplay between population dynamics and dispersal. One can think of scenarios in which a well-mixed population has a primitive matrix but spatial heterogeneity and limited dispersal lead to a spatial operator which is not u_0-positive. Vice versa, one can think of a population on isolated sites that has reducible matrices, yet given sufficient dispersal between the sites, the operator of the spatial model can be irreducible.

Our hope is that the results in this paper will lay the foundation for detailed analysis of population persistence in explicitly fragmented habitats. As such, the model and its conclusions should be compared to other model types, for example individual-based models or spatially-explicit stochastic models [8]. As the population size decreases, we expect stochastic events to play an important role. We also expect the average dispersal success to be helpful for other types of spatial models such as metapopulation models [10]. There, it is usually assumed that habitat patches are small relative to their distance to other patches, and that dispersal between patches follows a negative exponential function of the distance. The average dispersal success is based on individual movement assumptions and gives a more detailed description of dispersal between patches.

Acknowledgements. MAL gratefully acknowledges support from National Science Foundation grant DMS 9973212, support from the Canada Research Chairs program, and an NSERC operating grant. Thanks to Alan Hastings for helpful discussions. Thanks to Odo Diekmann for pointing out the need for the corrected proof of inequality (16) in a previous paper [32]. We are very thankful for very detailed comments from three referees, who helped us improve the paper.

A. Appendix

A.1. Table of frequently used symbols

$u = (u_1, \dots, u_m)$	density of a population with m stages
u^*	density at equilibrium
$\bar{u}$	spatial average of u^*
B, b	per capita birth rate for structured/scalar population
F, f	total production for structured/scalar population
Ω, Ω_α	(component of) habitat
K, k, k_{ij}	(matrix of) dispersal kernels
S, s, s_{ij}	(matrix of) dispersal success functions
$\hat{S}, \hat{s}$	(matrix of) average dispersal success
R, r_{ij}	(matrix of) redistribution functions
$\mathcal{A}, \mathcal{D}$	integrodifference operator, linsarization
λ	leading eigenvalue of $\mathcal{D}$
$\phi = (\phi_1, \dots, \phi_m)$	(eigen-) function in linearization
P	population growth parameter
L	domain length measure
σ^2	variance of dispersal kernel
U^α	average of u on patch Ω_α
B^α	the (constant) birthrate on patch Ω_α
$S^\alpha(x)$	dispersal success from x into patch Ω_α
$S^{\alpha\beta}$	Average dispersal success from patch Ω_β into Ω_α

A.2. Examples to Proposition 4

In the scalar case, the condition that $f(u) = b(u)u$ is monotone and concave can be written in terms of b as $-b(u) \leq b'(u)u \leq 0$. In the vector-valued case, if we assume all production rates to be smooth we can write conditions (13), (14) as $\partial_k b_{ij} \leq 0$ for all i, j, k and

$$\sum_j \partial_k b_{ij}(u) u_j \geq -b_{ik}(u). \tag{57}$$

Hence, we get lower bounds for the partial derivatives. In particular, if for some i, k we have $b_{ik} = 0$ then necessarily $\partial_k b_{ij} = 0$ for all j. This means, if stage k does not produce stage i then all the production rates b_{ij} are independent of stage k. In particular, the b_{ij} cannot depend on the total population in that case.

We consider an age-structured model with Leslie matrix

$$B = \begin{pmatrix} b_1 & b_2 & b_3 & \dots & b_m \\ \sigma_1 & 0 & 0 & \dots & 0 \\ 0 & \sigma_2 & 0 & & 0 \\ \vdots & \vdots & \ddots & \ddots & \vdots \\ 0 & \dots & & \sigma_{m-1} & 0 \end{pmatrix}. \tag{58}$$

By the remark above, the survival rate σ_j can depend only on the age class u_j. The condition on σ_j for monotonicity and concavity then reduces to the one-dimensional condition

$$-\sigma_j(u_j) \leq \sigma_j'(u_j) u_j \leq 0 \quad \text{for all} \quad j. \tag{59}$$

If each birth rate b_j depends only on u_j then conditions (13), (14) become the one-dimensional condition as well. If each b_j depends on the total population, then the conditions read

$$\sum_j b_j'(\tilde{u}) u_j \geq -\sup_k b_k(\tilde{u}) \quad \text{where} \quad \tilde{u} = \sum_j u_j. \tag{60}$$

If b_j depends on some weighted sum, then the condition is

$$w_k \sum_j b_j'(\hat{u}) u_j \geq -b_k(\hat{u}) \quad \text{for all} \quad k, \quad \text{where} \quad \hat{u} = \sum_j w_j u_j \tag{61}$$

The Beverton-Holt model for a single population is $b(u) = \alpha/(1 + \beta u)$. We use this functional for each b_j, i.e.,

$$b_j(\tilde{u}) = \frac{\alpha_j}{1 + \beta_j \tilde{u}}. \tag{62}$$

In the special case $\beta_j = 1$ for all j we can write out the conditions above as

$$\sum_{j \neq k} \frac{\alpha_j u_j}{(1 + \tilde{u})^2} + \frac{\alpha_j}{1 + \tilde{u}} \left(\frac{u_k}{1 + \tilde{u}} - 1 \right) \leq 0. \tag{63}$$

This leads to

$$\sum_{j \neq k} (\alpha_j - \alpha_k) u_j - \alpha_k \leq 0, \tag{64}$$

from which we see that necessarily $\alpha_j = \alpha_k$ for all k, j. Hence, the case of equal birth rates $b_j(\tilde{u}) = \alpha/(1+\tilde{u})$ satisfies the condition for existence of a unique fixed point. In case the b_j depend on the weighed sum (61), i.e.,

$$b_j(\hat{u}) = \frac{\alpha_j}{1+\hat{u}}, \tag{65}$$

the condition reads

$$\sum_j \frac{\alpha_j w_k u_j}{(1+\hat{u})^2} \leq \frac{\alpha_k}{1+\hat{u}}, \tag{66}$$

which gives

$$\sum_j (w_k \alpha_j - w_j \alpha_k) u_j \leq \alpha_k. \tag{67}$$

Assuming all weights are positive, this condition is satisfied if

$$\frac{w_j}{w_k} = \frac{\alpha_j}{\alpha_k}. \tag{68}$$

This means that classes have to be weighted exactly according to their "productivity"-parameter α_j.

A.3. Proofs

Proof of Theorem 1. We first show that if B^n is positive for some non-negative matrix B, then B^{n+1} is positive and hence, B^{n+l} is positive for all $l \geq 0$. The i, j-entry of B^{n+1} is

$$\sum_{l=1}^{m} b_{il} \left(\sum_{h_1=1}^{m} \cdots \sum_{h_{n-1}=1}^{m} b_{lh_1} \dots b_{h_{n-1}j} \right). \tag{69}$$

By assumption, the terms in brackets are all positive. If the i, j-entry of B^{n+1} was zero, then necessarily $b_{il} = 0$ for $l = 1...m$. But this implies that the ith row of any power of B is zero, which is a contradiction.

Since the b_{ij} are continuous and the domain is compact, one can choose the power n such that $B^n(0, y)$ is positive independently of y.

Taking powers of $\mathcal{D}$ and using Fubini's Theorem, we compute the i-entry

$$\begin{aligned}(\mathcal{D}^N \phi(x))_i = \int \cdots \int \sum \cdots \sum k_{i,l_1}(x, y_1) \dots k_{l_{N-1}j}(y_{N-1}, y_N) \\ \times b_{i,l_1}(y_1) \dots b_{l_{N-1}j}(y_N) \phi_j(y_N) dy_1 \dots dy_N.\end{aligned} \tag{70}$$

We choose N large enough such that B^N is positive. By assumption (A3), for each pair (i, j), at least one of the products of the entries of B in (70) is positive. Also, from (A3) and continuity of B we get a lower bound $b_{ij} \geq b_{\min} > 0$ for all nonzero

b_{ij}. By assumption, all the kernels are bounded above and below. Hence, we get the estimate

$$(\underline{\kappa} b_{\min})^N \int \phi(y)dy \le \mathcal{D}^N \phi(x) \le mN(\overline{\kappa} b_{\max})^N \int \phi(y)dy. \qquad (71)$$

Therefore, $\mathcal{D}$ is u_0-positive with $u_0 = 1$ (see 2.1 in [20]). Then by Thm. 2.5 [20] there is at least one positive eigenvalue with non-negative eigenvector Φ of $\mathcal{D}$. The positive cone in $\mathcal{L}^2$ is reproducing, and so by Thm. 2.10, the eigenvalue is simple. By Thm. 2.13, it is also dominant. Furthermore, by Thm. 2.11 no other eigenvector is in the positive cone. It remains to show that the eigenvector Φ is positive. Suppose that there is a set Ω_0 of positive measure on which the i-th component of Φ is zero. Then for sufficiently large n we find

$$0 = (\lambda^n \Phi_i(x))_{|\Omega_0} = (\mathcal{D}^n \Phi(x))_{i|\Omega_0} > 0, \qquad (72)$$

by (70), which is a contradiction. □

Proof of Proposition 1. We first assume that the set Ψ contains an open neighborhood of the diagonal in Ω^2, i.e., using assumption (A4) we find an $\varepsilon > 0$ such that for all nonzero kernels we get

$$k_{ij}(x, y) \ge \underline{\kappa} \quad \text{for} \quad |x - y| \le \varepsilon. \qquad (73)$$

For a connected bounded habitat, there is a number N_0 such that each point is connected to each other point by a path of length less than N_0. The mathematical expression for that fact is given by the N_0-fold iteration of nonzero kernels being positive:

$$k_{N_0}(x, y) = \int \cdots \int k_{ij}(x, y_1) \ldots k_{hl}(y_{N_0}, y)dy_1 \ldots dy_{N_0} \ge \underline{\kappa}^{N_0}. \qquad (74)$$

Now choose $N \ge N_0$ such that B^N is positive. Then, as above, one of the products of the entries of B in (70) is positive and by assumption (A2) and (74) the corresponding product of the kernels is also positive. Hence we get the estimate (71) and the proof continues as above.

For arbitrary Ψ we observe that for all $x \in \Omega$ by symmetry

$$\kappa_2(x, x) = \int \kappa(x, y)\kappa(y, x)dy = \int \kappa(x, y)\kappa(x, y)dy \ge \underline{\kappa}\delta > 0. \qquad (75)$$

By continuity then, κ_2 is positive for $|x - y|$ small enough. Hence, using twice as many iterations we are back to the first case. □

Proof of Proposition 2. We first prove this proposition under the assumption that there is only one stage, and that the kernel is continuous. The idea is that, given $x \in \Omega_\alpha$ and $y \in \Omega_\beta$, we find a sequence of points $y = z_1, \ldots, z_N = x$ such that $k(z_i, z_{i-1}) > 0$. We call such a sequence a connecting path. Then $\mathcal{D}^N$ satisfies inequalities (71) and hence $\mathcal{D}$ is superpositive.

Without loss of generality we can assume that the kernel k is positive in some neighborhood of the diagonal of each Ω_α^2. First, we use primitivity of C to find a sequence $\beta = \gamma_1, \ldots, \gamma_n = \alpha$ such that $c_{\gamma_{i+1}\gamma_i} = 1$. This gives a sequence of points $y_i \in \Omega_{\gamma_i}$ and $x_{i+1} \in \Omega_{\gamma_{i+1}}$ such that $k(x_{i+1}, y_i) > 0$. On each component Ω_{γ_i} we apply Proposition 1 to find a sequence $x_i = y_i^0, \ldots, y_i^{N_i} = y_i$ with $k(y_i^{j+1}, y_i^j) > 0$. Since Ω is compact, there exists a number N_0 such that for any $x, y \in \Omega$ a connecting path can be chosen with length at most N_0.

In the case of $m > 1$ stages one combines the idea above with primitivity of B as in Theorem 1. In the case that the kernels are not continuous one defines the connectivity matrix C as follows:

$$c_{\alpha\beta} = 1 \quad \text{if} \quad \int_{\Omega_\alpha} \int_{\Omega_\beta} k_{ij}(x, y) b_{ij}(0, y) dy dx > 0 \tag{76}$$

for some i, j. Then the same arguments work. □

Proof of Lemma 2. By assumption, we have $B(0, y; Q) \geq B(0, y; P)$. Hence, $\mathcal{D}^n(Q) \geq \mathcal{D}^n(P)$ and so $\lambda(Q) \geq \lambda(P)$. We establish that in fact $\lambda(Q) > \lambda(P)$. We write

$$\mathcal{D}(Q)\psi(x) = \mathcal{D}(P)\psi(x) + \int [K(x, y) \circ (B(0, y; Q) - B(0, y; P))]\psi(y) dy. \tag{77}$$

Iterating, we get

$$\mathcal{D}^n(Q) = \mathcal{D}^n(P) + C(Q, P) \tag{78}$$

for some linear operator $C(Q, P) \geq 0$. Then

$$\begin{aligned} \lambda^n(Q)\phi(\cdot; Q) &= \mathcal{D}^n(Q)\phi(\cdot; Q) \\ &= \mathcal{D}^n(P)\phi(\cdot; Q) + C(Q, P)\phi(\cdot; Q) \\ &= \mathcal{D}^n(P)\phi(\cdot; Q) + f, \end{aligned} \tag{79}$$

where f is positive (see Theorem 1). For sufficiently large n we have

$$\mathcal{D}^n(P) f \geq \varepsilon \phi(\cdot; P) \tag{80}$$

for some $\varepsilon > 0$. Then by Thm. 2.16 in [20] the equation

$$\lambda(Q)\psi = \mathcal{D}(P)\psi + f \tag{81}$$

does not have a solution for $\lambda(Q) \leq \lambda(P)$. But since $\phi(\cdot; Q)$ is a solution by construction, we necessarily have $\lambda(Q) > \lambda(P)$. This completes the proof of Lemma 2 (a).

We now formulate Lemma 2 (b) in greater generality. Suppose two domains $\Omega_1, \Omega_2 \subset \mathbb{R}^n$ are given, with $\Omega_1 \subset \Omega_2$, such that $\Omega_2 \backslash \Omega_1$ has nonempty interior. Denote by $\mathcal{D}_j$ the corresponding linear operators and by K_j their corresponding kernels.

(A8) Assume that on Ω_1, D_1 and D_2 share the same population projection matrix B and that the restriction of K_2 to Ω_1^2 equals K_1.

Then, the leading eigenvalue of $\mathcal{D}_2$ is strictly larger than the one of $\mathcal{D}_1$.

To prove the claim, we view $L^2(\Omega_1)$ as a subset of $L^2(\Omega_2)$. A function ρ on Ω_1 is extended to $\hat{\rho}$ on Ω_2 by setting it to zero on $\Omega_2\backslash\Omega_1$. On $L^2(\Omega_2)$ we define the cut-off operator Z in a similar way as

$$Z\psi(x) = \begin{cases} \psi(x) & x \in \Omega_1, \\ 0 & x \in \Omega_2\backslash\Omega_1. \end{cases}$$

We denote $\hat{\mathcal{D}}_1$ as the extension of $\mathcal{D}_1$ to $L^2(\Omega_2)$, i.e.

$$\hat{\mathcal{D}}_1\psi = \widehat{\mathcal{D}_1 Z\psi}. \tag{82}$$

In particular, for $\rho \in L^2(\Omega_1)$ we have

$$\widehat{\mathcal{D}_1\rho} = \hat{\mathcal{D}}_1 Z\hat{\rho}. \tag{83}$$

Then we may write for $\psi \in L^2(\Omega_2)$,

$$\begin{aligned} \mathcal{D}_2\psi &= [Z + (I - Z)]\mathcal{D}_2[Z + (I - Z)]\psi \\ &= Z\mathcal{D}_2Z\psi + Z\mathcal{D}_2(I - Z)\psi + (I - Z)\mathcal{D}_2Z\psi + (I - Z)\mathcal{D}_2(I - Z)\psi \\ &= Z\mathcal{D}_2Z\psi + G_1\psi, \end{aligned} \tag{84}$$

where G_1 is the sum of operators containing $(I - Z)$. Due to assumption (A8), we find that $Z\mathcal{D}_2Z = \hat{\mathcal{D}}_1$. Equation (84) is has a form similar to (77), and we proceed similarly as above. The positive eigenfunction ϕ of $\mathcal{D}_2$ to the eigenvalue λ_2 satisfies

$$\lambda_2^n\phi = \hat{\mathcal{D}}_1^n\phi + G_2\phi, \tag{85}$$

where G_2 is some linear operator. In the definition of the domain in 3.1, we assumed that points at which the species cannot settle and reproduce are excluded from $\Omega_{1,2}$. Therefore, the operator G_2 is positive. The claim follows as above.

Obviously, the claim of Lemma 2 (b) as stated in the main text follows from the above. The condition $K(x, y) = K(x - y)$ insures that the kernel on the smaller domain is simply the restriction of the kernel on the larger domain. The general formulation of the lemma applies in particular to families of domains of fixed shape with one size parameter L. □

Proof of Lemmas 4 and 5. We denote the positive eigenvector of $\mathcal{D}$ by Φ. The inner product on $\mathcal{L}^2$ is given by

$$\langle\phi, \psi\rangle = \int \phi^T(x)\psi(x)dx. \tag{86}$$

Then the adjoint operator of $\mathcal{D}$ is

$$\mathcal{D}^*\psi(y) = \int [K^T(x, y) \circ B^T(0, y)]\psi(x)dx. \tag{87}$$

The operator $\mathcal{D}^*$ is superpositive if $\mathcal{D}$ is, we denote the corresponding positive eigenvector by Ψ.

Fixing L, the operator $\mathcal{A}$ can be written as

$$\begin{aligned}\mathcal{A}(P)(u) = \mathcal{D}(P^*)u + \mathcal{B}(P^*)u(P - P^*)\\ +\mathcal{C}(P^*)(u) + o(\|u\|^2, |P - P^*|),\end{aligned} \tag{88}$$

where the linear operator $\mathcal{B}$ is given by

$$\mathcal{B}(P^*)u = \int [K(x, y) \circ \frac{\partial}{\partial P} B(0, y; P^*)]u(y)dy, \tag{89}$$

and the quadratic form $\mathcal{C} = (\mathcal{C}_1, ..., \mathcal{C}_m)$ has entries

$$\mathcal{C}_i(P^*)(u) = \int u^T (DB_i)udy, \tag{90}$$

where the l, j-th entry of the matrix DB_i is given by

$$(DB_i)_{lj} = k_{ij}(x, y)\frac{\partial}{\partial u_l} b_{ij}(0, y; P^*). \tag{91}$$

Following the argument 56.5 in [21] we have to show the following two conditions: $\langle \mathcal{B}(P^*)\Phi_0, \Psi_0\rangle > 0$ and $\langle \mathcal{C}(P^*)\Phi_0, \Psi_0\rangle < 0$. The inner product

$$\langle \mathcal{B}(P^*)\Phi_0, \Psi_0\rangle = \int \sum_l \int \sum_j k_{lj}(x, y)\frac{\partial}{\partial P} b_{lj}(0, y; P^*)\Phi_{0j}(y)dy\, \Psi_{0l}(x)dx \tag{92}$$

is positive if all b_{lj} are non-decreasing in P and at least one b_{lj} is increasing in P. Similarly, the inner product $\langle \mathcal{C}(P^*)\Phi_0, \Psi_0\rangle$ is negative by assumption (A7). This completes the proof for fixed L.

Fixing P, we can write $\mathcal{A}(L)$ as in (88) with P, P^* replaced by L, L^*. The linear operator $\mathcal{B}$ is now given by

$$\mathcal{B}(L^*)u = \int [\frac{\partial}{\partial L} K(x, y; L) \circ B(0, y)]\, u(y)dy, \tag{93}$$

and $\mathcal{C}$ is just as above with the parameter L^* appearing in K and the parameter P^* deleted from B. We only have to show that $\langle \mathcal{B}(P^*)\Phi_0, \Psi_0\rangle > 0$. Rearranging (92) we write in coordinates

$$\int \sum_l \sum_j \left\{\frac{\partial}{\partial L} \int k_{lj}(x, y; L)\Psi_{0l}(x)dx\right\} b_{lj}(0, y)\Phi_{0j}(y)dy\, \Psi_{0l}(x)dx. \tag{94}$$

Since Ψ_0 is positive, the assumptions on the dispersal success functions also hold for the weighed dispersal success

$$s^{\Psi}_{lj}(y; L) = \int k_{lj}(x, y; L)\Psi_{0l}(x)dx, \tag{95}$$

and hence, the inequality holds. □

Proof of Lemma 7. Since $\mathcal{D}_1$ is completely continuous and $\mathcal{D}_2$ is continuous, both products $\mathcal{D}_1\mathcal{D}_2$ and $\mathcal{D}_2\mathcal{D}_1$ are completely continuous. The power of $\mathcal{D}$ can be written as a sum of products of $\mathcal{D}_1$ and $\mathcal{D}_2$,

$$\mathcal{D}^n = \mathcal{D}_1^n + \mathcal{D}_1^{n-1}\mathcal{D}_2 + \mathcal{D}_1^{n-2}\mathcal{D}_2\mathcal{D}_1 \cdots + \mathcal{D}_2^{n-1}\mathcal{D}_1 + \mathcal{D}_2^n, \tag{96}$$

and the last term vanishes for $n \geq n_0$, such that $\mathcal{D}^n$ is completely continuous. Hence, all nonzero points in the spectrum of $\mathcal{D}^n$ are eigenvalues of finite multiplicity. Therefore, by the spectral mapping theorem all nonzero points in the spectrum of $\mathcal{D}$ are eigenvalues of finite multiplicity.

Assumptions (A1–4) ensure positivity of some sufficiently high power of $\mathcal{D}$ in the same way as they did in Proposition 1, so that $\mathcal{D}^n$ is superpositive for some n. Denote by μ the simple dominant positive eigenvalue of $\mathcal{D}^n$ with unique positive eigenvector ψ. Denote by λ any eigenvalue of $\mathcal{D}$ which satisfies $\lambda^n = \mu$ and the corresponding eigenvector by ϕ. Then

$$\mu\phi = \lambda^n\phi = \mathcal{D}^n\phi \tag{97}$$

and hence by uniqueness $\phi = \psi$ (up to scalar multiples). Therefore λ has to be positive. Monotonicity of the power function implies $\mu > 1$ iff $\lambda > 1$ and also that λ is dominant. Finally, Theorem 2.10 in [20] gives that λ is simple. □

Proof of Lemma 8. The idea is the same as in the proof above. Due to nonlinearity one has to be somewhat more careful. We write

$$\mathcal{A}^n(u) = \mathcal{A}_1(\mathcal{A}^{n-1}(u)) + \mathcal{A}_2\mathcal{A}_1(\mathcal{A}^{n-2}(u)) + \cdots + \mathcal{A}^{n-1}\mathcal{A}_1(u) + \mathcal{A}^n u. \tag{98}$$

The last term vanishes since $\mathcal{A}_2$ is nilpotent, all other terms are compact. □

References

1. Andersen, M.: Properties of some density-dependent integrodifference equation population models. Math. Biosci. **104**, 135–157 (1991)
2. Botsford, L.W., Hastings, A., Gaines, S.D.: Dependence of sustainability on the configuration of marine reserves and larval dispersal distance. Ecology Letters **4**, 144–150 (2001)
3. Broadbent, S.R., Kendall, D.G.: The random walk of trichostrongylus retortaeformis. Biometrica **9**, 460–466 (1953)
4. Cantrell, R.S., Cosner, C.: Should a park be an island? SIAM Appl. Math **53**, 219–252 (1993)
5. Cantrell, R.S., Cosner, C.: On the effects of spatial heterogeneity on the persistence of interacting species. J. Math. Biol. **37**, 103–145 (1998)
6. Caswell H.: Matrix Population Models. Sinauer Associates, Sunderland, 2001
7. DeAngelis, D.L., Svoboda, L.J., Christensen, S.W., Vaughan, D.S.: Stability and return times of Leslie matrices with density-dependent survival. Ecol. Modeling **8**, 149–163 (1980)
8. Engen, S., Lande, R., Sæther, B.E.: Migration and spatiotemporal variation in population dynamics in a heterogeneous environment. Ecology **83**(2), 570–579 (2002)

9. Fagan, W.F., Cantrell, R.S., Cosner, C.: How habitat edges change species interaction. Am. Nat. **153**, 165–182 (1999)
10. Hanski, I., Ovaskainen, O.: The metapopulation capacity of a fragmented landscape. Nature **404**, 755–758 (2000)
11. Hardin, D.P., Takáč, P., Webb, G.F.: Asymptotic properties of a continuous-space discrete-time population model in a random environment. J. Math. Biol. **26**, 361–374 (1988)
12. Hardin, D.P., Takáč, P., Webb, G.F.: A comparison of dispersal strageties for survival of spatially heterogeneous populations. SIAM J. Appl. Math **48**, 1396–1423 (1988)
13. Hardin, D.P., Takáč, P., Webb, G.F.: Dispersion population models discrete in time and continuous in space. J. Math. Biol. **28**, 1–20 (1990)
14. Hastings A.: Personal communication, 2002
15. Henson, S.M., Cushing, J.M., Costantino, R.F., Dennis, B., Desharnais, R.A.: Phase switching in population cycles. Proc. Royal Soc., London B **265**, 2229–2234 (1998)
16. Kierstead, H., Slobodkin, L.B.: The size of water masses containing plankton blooms. J. Marine Res. **12**, 141–147 (1953)
17. Kot, M.: Discrete-time travelling waves: Ecological examples. J. Math. Biol. **30**, 413–436 (1992)
18. Kot M.: Elements of Mathematical Ecology. Cambridge Univ. Press, Cambridge, 2001
19. Kot, M., Schaffer, W.M.: Discrete-time growth-dispersal models. Math. Biosci. **80**, 109–136 (1986)
20. Krasnosel'skii M.A.: Positive Solutions of Operator Equations. Noordhoff LTD, Groningen, 1964
21. Krasnosel'skii M.A., Zabreiko P.P.: Geometrical Methods of Nonlinear Analysis. Springer Verlag, Berlin, 1984
22. Lefkovitch, L.P.: The study of population growth in organisms grouped by stage. Biometrics **21**, 1–18 (1965)
23. Leslie, P.H.: On the use of matrices in certain population mathematics. Biometrika **33**, 183–212 (1945)
24. Lui, R.: Existence and stability of traveling wave solutions of a nonlinear integral operator. J. Math. Biol. **16**, 199–220 (1983)
25. Neubert, M., Caswell, H.: Density-dependent vital rates and their population dynamic consequences. J. Math. Biol. **41**, 103–121 (2000)
26. Neubert, M.G., Caswell, H.: Demography and dispersal: Calculation and sensitivity analysis of invasion speeds for structured populations. Ecology **81**(6), 1613–1628 (2000)
27. Neubert, M.G., Kot, M., Lewis, M.A.: Dispersal and pattern formation in a discrete-time predator-prey model. Theor. Pop. Biol. **48**(1), 7–43 (1995)
28. Peters C.M.: Population ecology and management of forest fruit trees in Peruvian Amazonia. In: Anderson A. (ed.), Alternatives to deforestation. Columbia University Press, New York, 1990, pp. 86–98
29. Skellam, J.G.: Random dispersal in theoretical populations. Biometrika **38**, 196–218 (1951)
30. Stamps, J., Buechner, M., Krishnan, V.V.: The effects of edge permeability and habitat geometry on emigration from patches of habitat. Am. Nat. **129**, 533–552 (1987)
31. Strogatz S.H.: Nonlinear Dynamics and Chaos. Addison-Wesley, Reading, MA, 1994
32. Van Kirk, R.W., Lewis, M.A.: Integrodifference models for persistence in fragmented habitats. Bull. Math. Biol. **59**(1), 107–137 (1997)
33. Van Kirk, R.W., Lewis, M.A.: Edge permeability and population persistence in isolated habitat patches. Nat. Resource Modeling **12**, 37–64 (1999)
34. Veit, R.R., Lewis, M.A.: Dispersal, population growth, and the Allee effect: Dynamics of the house finch invasion in eastern North America. Am. Nat. **148**(2), 255–274 (1996)

35. Wang, M.H., Kot, M., Neubert, M.G.: Integrodifference equations, Allee effects, and invasions. J. Math. Biol. **44**, 150–168 (2002)
36. Weinberger, H.F.: Long-time behavior of a class of biological models. SIAM J. Math. Anal. **13**, 353–396 (1982)